

THE INFLUENCE OF Mg AND Mn CONTENT ON ABNORMAL GRAIN GROWTH IN AA5182 TYPE ALLOYS

Tamara Radetić^{1}, Miljana Popović¹, Bojan Gligorijević², Ana Alil², Endre Romhanji*

¹ University of Belgrade, Faculty of Technology and Metallurgy, Belgrade, Serbia

² University of Belgrade, Innovation Center of Faculty of Technology and Metallurgy, Belgrade, Serbia

Received 14.12.2019

Accepted 17.12.2019

Abstract

The occurrence of abnormal grain growth (AGG) in AA5182 alloy during annealing imposes severe restrictions on processing parameters and deteriorates mechanical properties. In this work, we investigated the effect of chemical composition on the appearance of abnormal grain growth by varying Mg and Mn content in the range of composition limits for standard AA5182 alloy, 4.0-5.0% Mg, and 0.2-0.5% Mn, respectively. Thermo-mechanical processing of alloys included cold rolling with reductions ranging from 40 to 85%, followed by annealing in the temperature range from 350 to 520 °C. The results showed that the rise in alloying elements content drives the onset of abnormal grain growth toward higher temperatures. The increase in the cold rolling reduction degree promotes abnormal grain growth and lowers its onset temperature. Abnormal grain growth and grain boundary mobility showed strong anisotropy related to rod-like shape and alignment of Al₆Mn(Fe) dispersoids through Zener pinning.

Keywords: abnormal grain growth; thermo-mechanical processing; AA5182 alloy.

Introduction

The current design of Al alloys is, in a significant part, directed toward modification and improvement of properties of existing alloys. An example is “traditional” Al-Mg alloy AA5182, where improvement of mechanical properties can lead to the introduction of new qualities and expansion of its applications in the transportation industry [1]. However, the propensity of the alloy toward abnormal grain growth (AGG) severely limits the annealing temperature range and its capability for hot forming [2]. AGG - duplex grain size distribution, i.e., development of microstructure

* Corresponding author: Tamara Radetić, tradetic@tmf.bg.ac.rs

consisting of large grains surrounded by finer, severely deteriorates mechanical properties of the alloy.

Despite a vast number of studies on recrystallization and grain growth mechanisms, there is still ongoing research in fundamental aspects of the phenomena as well as in practical interest in the development of new processing routes [3-6]. Some key aspects, such as initiation and mechanisms of AGG, remained unresolved [3]. In metal materials, AGG occurs when particles, texture, or surface effects inhibit normal grain growth, and some grains have a growth advantage over neighboring grains [7].

Studies of particle-containing aluminum alloys [8-11] showed that the occurrence of AGG strongly depends on the annealing temperature. The AGG tends to take place at temperatures just below the solvus characterized by high grain boundary mobility and a relatively small volume fraction of pinning particles. Role of texture is highlighted in the studies on low-alloyed Al-alloys with insignificant dispersoid fraction [12-15].

A few studies [8, 9] reported observations of the AGG in AA5182 alloys at temperatures above 480 °C even though with different kinetics. According to both studies, AGG was caused by dispersoid coarsening and dissolution, whereas its initiation was attributed to the size advantage of grains with specific texture components [8].

This study is aimed to investigate whether minor variation in the chemical composition of AA5182 alloys, while staying in the range of composition limits defined by the standard, affects AGG. The influence of thermo-mechanical processing parameters such as degree of cold rolling reduction and annealing temperature on the appearance of AGG was systematically characterized in order to develop a strategy for avoiding AGG during high temperature anneal.

Experimental procedure

Four alloys, with chemical compositions within a range defined by the standard for AA5182 alloy (Table 1), were characterized after undergoing the same thermo-mechanical treatment to evaluate whether minor compositional variations influence the occurrence of abnormal grain growth.

Table 1. Chemical composition of the AA5182 type alloys, mass%

Alloy	Mg	Mn	Si	Fe	Ti	Cu	Zn	Cr	Rest
Standard	4.0-5.0	0.2-0.5	≤ 0.2	≤ 0.35	≤ 0.1	≤ 0.15	≤ 0.25	≤ 0.1	≤ 0.15
A	4.04	0.371	0.073	0.186	0.002	0.011	0.022	0.011	0.008
B	4.47	0.249	0.078	0.166	0.007	0.016	0.001	0.041	0.006
C	4.16	0.470	0.149	0.288	0.009	0.008	0.018	0.060	0.003
D	4.88	0.500	0.143	0.376	0.013	0.030	0.071	0.105	0.051

The alloy A had low Mg content and moderate amounts of dispersoid forming elements such as Fe, Mn, and Cr. The alloy B had medium Mg content, but Fe and Mn close to the lower limit prescribed by the standard. Alloys C and D were low and high in Mg, respectively, but contained a higher fraction of dispersoid forming elements. All four alloys were provided by Impol Seval Aluminium Mill company. The industrial processing of the alloys included direct chill (DC) casting, homogenization at 550 °C and hot rolling.

Thermo-mechanical processing of the as-received material included cold rolling to reductions in a range from 40 to 85 % followed by annealing at 350-520 °C for 1 h (Table 2). Additionally, specimens of alloy A cold rolled 64 % were isothermally annealed at 480 °C for various times ranging from 5 min to 180 min.

Table 2. Annealing conditions after cold rolling. Specimens were annealed for 1 h.

Cold rolling reduction, %	Annealing temperature, °C						
	350	400	440	470	480	500	520
40							
60							
85							

The microstructure of as-received and processed material was characterized by optical microscopy (OM) under polarized light and scanning electron microscopy (SEM) in FEG SEM Tescan Mira at 20 kV. Specimens in longitudinal cross-section, i.e. rolling-normal (RD-ND) orientation, were mechanically polished and electrolytically etched in Barker's reagent. Composite images of the large specimen areas were created by digitally stitching together individual micrographs. Image processing and analysis were conducted using ImageJ software.

Results

Grain microstructure characterization showed that the AGG tends to follow primary recrystallization during the annealing at temperatures above 400 °C in AA5182 type alloys. For example, the microstructure of alloy A was fully recrystallized upon reaching an annealing temperature of 480 °C. There was a grain size gradient throughout the specimen thickness, which is typical for rolled material. However, there was no evidence of enlarged grains that would point out at the start of AGG. Annealing at 480 °C for 5 min resulted in the appearance of grains larger than average in the region up to 700 µm from the plate surface (Fig. 1a).

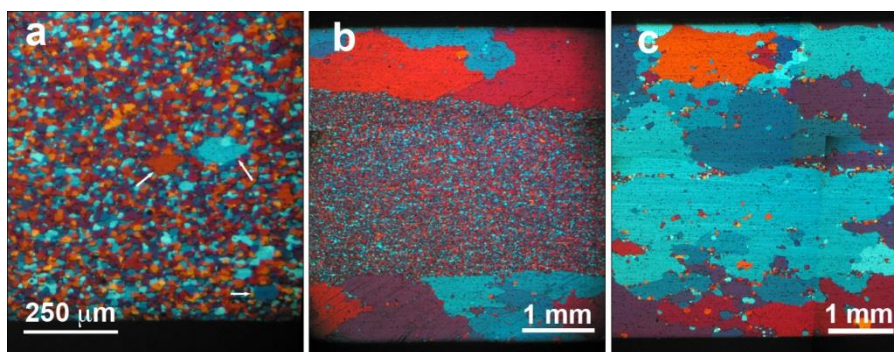


Fig. 1. OM. Evolution of the grain microstructure in 60 % cold rolled alloy A during annealing at 480 °C for: (a) 5 min anneal; (b) 30 min anneal; (c) annealing for 1 h at 520 °C.

Further annealing led to AGG and formation of a sandwich-like microstructure consisting of two bands of abnormally large grains enclosing fine-grained material in

the center of the plate (Fig. 1b). In contrast to excessive grain growth in outer parts of the plate, the mean grain size in the plate center changed a little, from 14.5 μm upon reaching annealing temperature of 480 $^{\circ}\text{C}$ to 17.7 μm after 1 h of annealing. Prolonged annealing and/or annealing at the higher temperatures can result in AGG throughout the plate with abnormal grains originating even in the central section of the plate (Fig. 1c). The microstructure (Fig. 1c) might evolve to consist of huge grains although with normal size distribution; however, residual clusters of fine grains and island grains point out that such morphology has been a result of abnormal grain growth.

The chemical composition of the alloy had a strong influence on the onset and extent of the abnormal grain growth. Fig. 2 illustrates this effect. In alloy A, annealing at 480 $^{\circ}\text{C}$ for 1 h after 60% cold rolling reduction resulted in the formation of sandwich-like microstructure (Fig. 2a), while in alloy B, characterized by the low level of dispersoid forming elements, abnormal grain growth encompassed the whole plate after the same thermo-mechanical treatment (Fig. 2b). Furthermore, alloy A did not exhibit AGG after annealing at 440 $^{\circ}\text{C}$ for 1 h, but in B, after the same treatment, two bands of abnormal grains were formed. In contrast, in alloy C, rich in dispersoid forming elements Fe and Mn (Table 1), the same thermo-mechanical treatment did not give rise to abnormal grain growth (Fig. 2c). Similarly, in the alloy D, high in Fe and Mn as well as Mg content, no abnormal grain growth was observed.

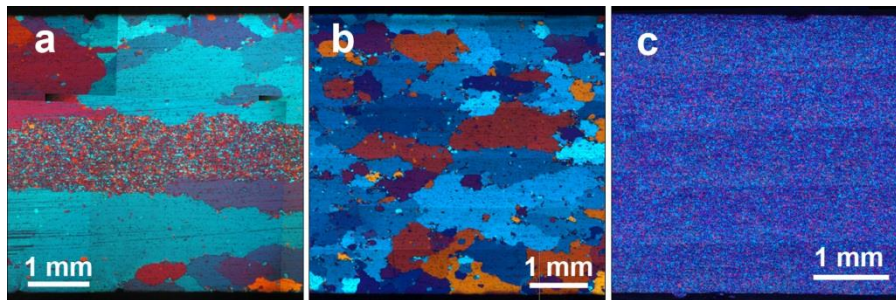


Fig. 2. OM. Influence of chemical composition on grain microstructure evolution in 64 % cold-rolled alloys during annealing for 1 h at 480 $^{\circ}\text{C}$: (a) alloy A; (b) alloy B; (c) alloy C.

Table 3. Progression of abnormal grain growth and abnormal grain parameters in alloys A and B after annealing at 440 $^{\circ}\text{C}$ and 480 $^{\circ}\text{C}$ for 1 h.

Alloy	Annealing temperature, $^{\circ}\text{C}$	Normal. Area*, mm^2/mm	<Eq. diameter>, μm	<Round.>	<Aspect ratio>
A	440	0.00	/	/	/
	480	1.63	743	0.45	2.7
B	440	0.91	528	0.51	2.0
	480	> 2.35	413	0.55	2.0

* The normalized area was calculated as the area covered by abnormal grains per unit length in RD. It corresponds to the mean length of propagation in front of abnormal grain growth in ND.

The effect of the chemical composition and, especially, dispersoid forming elements on the boundary mobility of abnormal grains is clear from the data in Table 3. The mean

propagation length of the abnormal growth front, in the direction normal to the plate surface, was higher for the alloy B, which is low in dispersoid forming elements, than for the A. The elongated shape of abnormal grains with longer axis parallel to the rolling direction (Figs. 1 and 2), as well as higher aspect ratio (Table 3), indicate anisotropy in the grain growth. Such a trend will be unexpected if the only controlling factor is capillary pressure, i.e. decrease in the interface area. Once the band of abnormal grains forms, the migration of the abnormal grain boundaries in the normal direction reduces total grain boundary area by consuming small grains; on the other hand, the migration of the boundaries parallel to rolling direction leaves total boundary area effectively unchanged until complete collapse of the intermediate abnormal grain. Likely cause for the anisotropy in grain mobility is anisotropic shape and alignment of the $Al_6Mn(Fe)$ particles (Fig. 3a) that can limit mobility through Zener pinning [16]. The particles pin more effectively segments of the boundary parallel to their long axis.

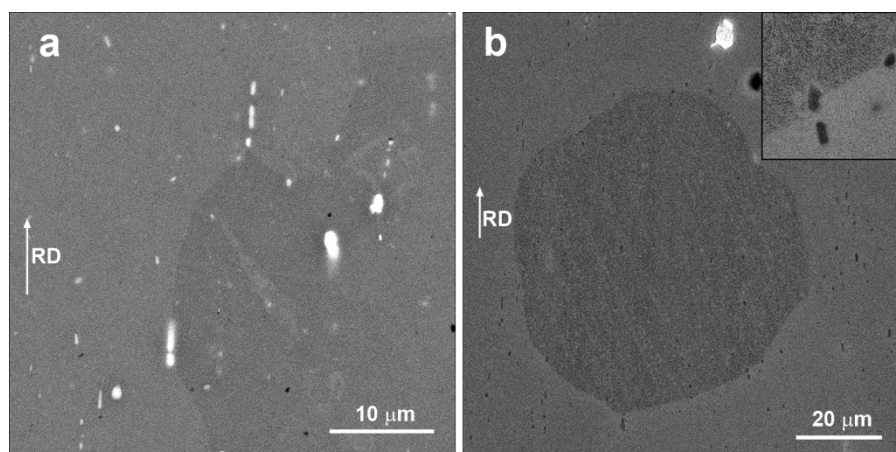


Fig. 3 (a) SEM micrograph of the rod-like $Al_6Mn(Fe)$ particles at the grain boundaries. The micrograph is of the boundary between two abnormal grains in the alloy A after annealing at 480 °C for 1 h. (b) SEM micrograph of the island grain within the abnormal grain in the alloy A. Insert shows the pinning of the boundary by dispersoids. The specimen was etched by Barker's reagent after annealing at 520 °C for 1 h.

Zener pinning might be responsible for greater stability and fraction of island grains (Fig. 3b) and fine grain clusters in alloys containing higher levels of Fe and Mn. Observations indicate that the alloy A is characterized by a higher fraction of island grains and clusters of fine grains within abnormal grains than the alloy B.

An increase in cold reduction from 60% to 85% initiated AGG in alloy C during the annealing at 480 °C for 1 h (Fig. 4a). The increase of the annealing temperature to 520 °C after 85 % reduction led to the AGG throughout the plate thickness. However, in the case of highly alloyed alloy D, neither high temperature nor high cold reduction initiated AGG (Fig. 4b). That could be due to the high Mg and its effect on recovery and recrystallization processes as well on suppressing mobility of grain boundaries.

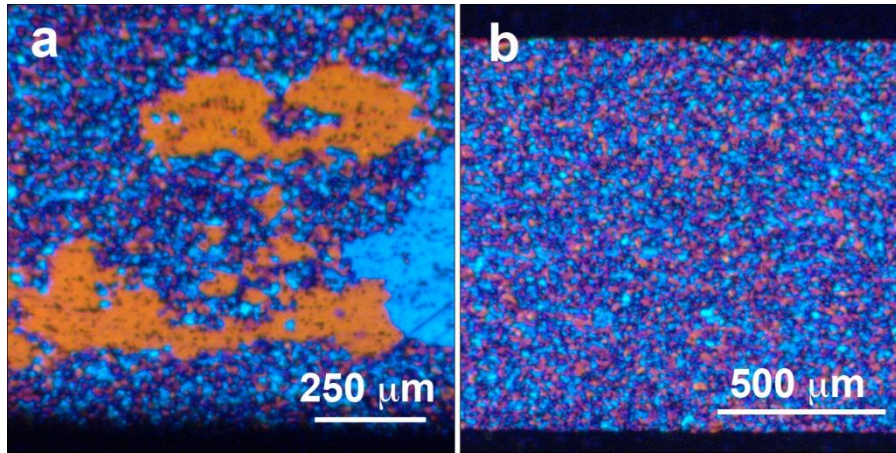


Fig. 4. OM. (a) The microstructure of the alloy C after 85 % cold reduction and annealing 1 h at 480 °C; (b) microstructure of the alloy D after 85 % cold reduction and annealing 1 h at 520 °C.

Table 4. Summary of the effect of chemical composition, cold rolling reduction and temperature on the occurrence of AGG and normal growth (NG).

Annealing temperature, °C	Alloy	Cold rolling reduction, %		
		40 %	60 %	85 %
440	A	NG	NG	AGG-start
	B	NG	AGG-band	AGG-whole
	C	NG	NG	NG
	D	NG	NG	NG
480	A	NG	AGG-band	AGG-whole
	B	AGG-start	AGG-whole	AGG-whole
	C	NG	NG	AGG-start
	D	NG	NG	NG
520	A	AGG-band	AGG-whole	AGG-whole
	B	AGG-whole	AGG-whole	AGG-whole
	C	NG	NG	AGG-whole
	D	NG	NG	NG

The influence of cold reduction and alloy chemical composition on the temperature of the onset and extent of AGG is summarized in Table 4. There is an inverse relationship between the degree of cold reduction and the onset temperature for AGG. For example, in the case of alloy A, after the cold reduction of 85 % AGG starts at 440 °C, but lowering reduction to 40 % shifts onset temperature to 500 °C [17]. Furthermore, it was observed that with an increase in cold reduction, incipient abnormal grains form deeper toward the plate center.

The two-stage annealing experiment illustrates that the number of factors controls the onset of AGG. The treatment involving low-temperature anneal at 220 °C for 48 h followed by high-temperature anneal for 1 h showed that the onset of AGG could be suppressed and shifted to longer annealing times. Single-stage annealing at 480 °C for 1 h led to the formation of bands of abnormal grains in the alloy A while in the B

abnormal growth progressed throughout the specimen (Figs. 2a and b). Furthermore, during annealing at the temperature as low as 440 °C the band was formed in the alloy B. After the two-stage treatment, neither microstructure of the alloy A after annealing at 480 °C nor the alloy B after annealing at 440 °C showed any abnormal grain growth (Fig. 5a). However, annealing at 480 °C resulted in the formation of a band of abnormal grains in alloy B (Fig. 5b).

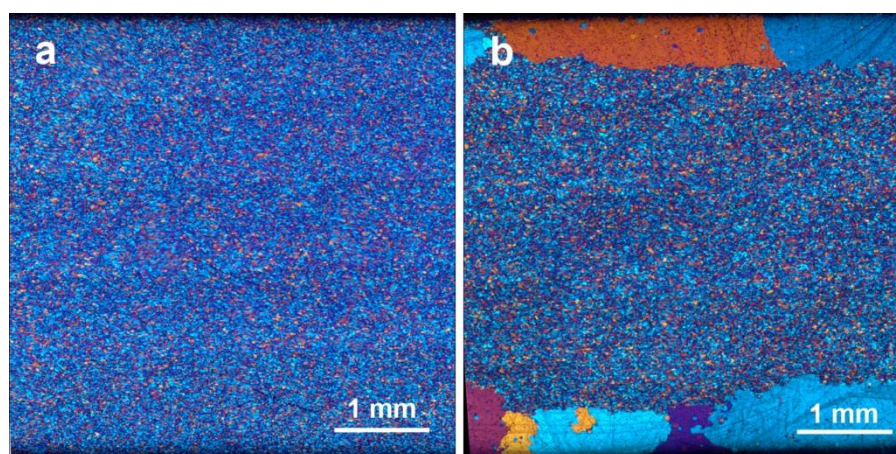


Fig. 5. OM. Grain microstructure of the alloy B after 60 % cold rolling reduction and two-stage annealing: (a) annealing at 220 °C for 48 h + 440 °C for 1 h; (b) annealing at 220 °C for 48 h + 480 °C for 1 h.

Discussion

The results summarized in Table 4 show that compositional variations, even within a range prescribed by the standard for AA5182 alloy, affect occurrence and kinetics of abnormal grain growth. It appears that higher content of dispersoid forming elements, Mn and Fe, shifts the onset of AGG to higher temperatures, and slows down propagation kinetics. According to some authors [8, 9], dispersoid coarsening and dissolution is responsible for AGG. However, this study showed that the AGG occurs at a 440 °C, while coarsening and dissolution is reported to be closer to 500 °C [8, 9]. This fact in conjunction with the greatest propensity toward AGG is a characteristic of the alloy with the lowest content of dispersoid forming elements. Thus, the smallest driving force for particle dissolution, points out that although dispersoids do decrease grain boundary mobility through Zener pinning, their coarsening and dissolution is not the key for the occurrence of the abnormal grain growth.

The strong influence of the degree of cold reduction on the onset temperature and extent of AGG observed in this study is similar to the findings reported in low-alloyed steel [19]. However, the explanation of the effect by higher dislocation density and fast diffusion paths for dissolution is unlikely in this case. In the reduction range of interest for this work, i.e. over 40%, the saturation with dislocations should be reached and a further increase in deformation is unlikely to boost diffusion significantly. Indeed, even for steel, onset temperature remained nearly constant in the reduction range 40-75% [18]. Moreover, the microstructure is already recrystallized upon reaching annealing

temperatures at which AGG takes place, so grains should be nearly dislocation free. The presence of recrystallized grains also rules out the “pinch-off” mechanism proposed by Taleff’s group [2].

Texture and special grain boundaries with high mobility are also considered as critical factors for AGG [7, 10]. The grain size gradient across the plate, a band of abnormal grains at the plate surface, and increasing depth of incipient abnormal grains with reduction as well as stable grains in the center suggest the role of texture gradient in the phenomena that need to be explored in the future work.

The effect of the two-stage annealing on AGG (Fig. 5) points out the role of subgrain boundaries. Activation of low-temperature recovery mechanisms during annealing at 220 °C can prevent high-temperature recovery and recrystallization by subgrain growth [6, 19]. The possibility that AGG is related to subgrain coalescence is supported by the morphology of growing grains in the early stage of abnormal grain growth (Fig. 4a). However, convoluted grain boundaries (Fig. 4a) also resemble the morphological features typical for the triple-junction wetting mechanism [20]. This mechanism of abnormal grain growth, based on energy considerations and solid-state wetting [20, 21], assumes that low-angle and subgrain boundaries of abnormal grains penetrate the matrix by repeated events of triple junction wetting. Although the exact mechanism of abnormal grain growth remains to be elucidated, the present study revealed the synergy of multiple factors on its onset and propagation.

Conclusions

Abnormal grain growth (AGG) in AA5182 type alloys is affected by multiple factors. Composition of the alloy, especially the content of dispersoid forming elements, appears to control the kinetics of abnormal grain growth through Zener pinning of grain boundaries by $Al_6(Mn, Fe)$ dispersoids. However, the onset and extent of AGG also strongly depend on parameters of thermo-mechanical processing such as degree of cold deformation and annealing temperature. The results show that lowering a reduction degree or two-stage annealing can suppress abnormal grain growth during annealing in a higher temperature range.

The preference of abnormal grains to form in the region close to the plate’s surface indicates that the initiation of AGG is controlled by texture and grain boundary character gradients. The anisotropy in the growth of abnormal grains is related to the shape and anisotropic alignment of $Al_6Mn(Fe)$ particles due to Zener pinning while grain morphology in the early stages of AGG and its suppression by two-stage annealing treatment points out on the role of recovery in the processes.

Acknowledgment

This work has been supported by the Ministry of Education, Science and Technological Development of the Republic of Serbia, and Impol Seval Aluminium Mill Sevojno, under contract No. TR34018.

References

- [1] J.R. T Hirsch: Nonferr Metal Soc, 24 (2014) 1995-2002.
- [2] J-K. Chang, K. Takata, K. Ichitani, E.M. Taleff: Metall Mater Trans, 41A (2010) 1942-1953.
- [3] P.R. Rios, D.Zöllner: Mater Sci Tech, 34 (2018) 629-638.
- [4] B.L. DeCost, E.A. Holm: Metall Mater Trans, 48A (2017) 2771-2780.
- [5] S.J. Hales, H.D. Claytor, J.A. Alexa, US Patent 9,090,950 (2015).
- [6] Q. Guo, X. Lei, R.E. Sanders Jr., X. Yang, Y. Liang, L. Wang, Z. Fan: Mater Sci Forum, 877 (2017) 264-271.
- [7] J. Humphreys, G.S. Rohrer, A. Rollett Recrystallization and related annealing phenomena 3rd ed. Elsevier, Amsterdam 2017. ISBN:978-0-08-098235-9
- [8] I. Samajdar, L. Rabet, B.Verlinden, P. van Houtte: Textures and Microstructures, 20 (1998) 191-206.
- [9] H.G. Suk, E.J. Shin, M.Y. Huh: Solid State Phenomena, 116-117 (2006) 316-319.
- [10] P.R. Rios, G. Gottstein: Acta Mater, 49 (2001) 1511-2518.
- [11] J. Dennis, P.S. Bate, F.J. Humphreys, Acta Mater, 57 (2009) 4539-4547.
- [12] H-C. Kim, C-G. Kang, M-Y. Huh, O. Engler: Scripta Mater, 57 (2007) 325-327.
- [13] O. Engler, M-Y. Huh: Mater Sci Eng A, 271 (1999) 371-381.
- [14] K. Matsumoto, T. Shibayanagi, Y. Umakoshi: Mater Trans JIM, 37 (1996) 1659-1664
- [15] B.B. Straumal, W. Gust, L. Dardiniier, J-L. Hoffmann, V.G. Sursaeva, L.S. Shvindlerman: Mater Des, 18 (1997) 293-295.
- [16] P.R. Rios, G.S. Fonseca: Scripta Mater, 50 (2004) 71-75.
- [17] T. Radetić, M. Popović, E. Romhanji (2020), accepted for publication in Mater. Tech.
- [18] X. Zhang, K. Matsuura, M. Ohno: Metals 8 (12) (2018)1004.
- [19] F.J. Humphreys: Acta Mater 45 (1997) 4231-4240.
- [20] H-K. Park, H-G. Kang, C-S. Park, M-Y. Huh, N-M. Hwang: Metal Mater Trans, 43A (2012) 5218-5523.
- [21] C-S. Park, T-W. Na, H-K. Park, D-K. Kim, C-H. Han, N-M. Hwang: Phil Mag Lett, 92 (2012) 344-351.



Creative Commons License

This work is licensed under a Creative Commons Attribution 4.0 International License.